Organometallic complexes for nonlinear optics
Part 25. Quadratic and cubic hyperpolarizabilities of some dipolar and quadrupolar gold and ruthenium complexes[☆]

Stephanie K. Hurst [a], Marie P. Cifuentes [a], Andrew M. McDonagh [a],
Mark G. Humphrey [a,*], Marek Samoc [b], Barry Luther-Davies [b], Inge Asselberghs [c],
André Persoons [c]

[a] *Department of Chemistry, Australian National University, Canberra, ACT 0200, Australia*
[b] *Laser Physics Centre, Research School of Physical Sciences and Engineering, Australian National University, Canberra, ACT 0200, Australia*
[c] *Laboratory of Chemical and Biological Dynamics, Centre for Research on Molecular Electronics and Photonics, University of Leuven, Celestijnenlaan 200D, B-3001 Leuven, Belgium*

Abstract

The complexes $[Au(4-C\equiv CC_6H_4NO_2)(L)]$ [L = PCy$_3$ (**1**), PMe$_3$ (**2**)], $[(L)Au(\mu-4-C\equiv CRC\equiv C)Au(L)]$ [R = C$_6$H$_4$, L = PCy$_3$ (**4**), PPh$_3$ (**5**); R = C$_6$H$_4$-4-C$_6$H$_4$, L = PCy$_3$ (**7**), PPh$_3$ (**8**)], *trans,trans*-[RuCl(dppm)$_2$(μ-4,4′-C$\equiv$CC$_6$H$_4$C$_6$H$_4$C$\equiv$C)RuCl(dppm)$_2$] (**11**), *trans*-[Ru(X)(Y)(dppe)$_2$] [X = Cl, Y = 4-C$\equiv$CC$_6$H$_4$I (**12**), 4-C$\equiv$CC$_6$H$_4$C$\equiv$CSiMe$_3$ (**13**); X = C$\equiv$CPh, 4-C$\equiv$CC$_6$H$_4$C$\equiv$CH (**14**)] and $\{$*trans*-[Ru(C$\equiv$CPh)(dppe)$_2$]$\}_2$(μ-4,4′-C$\equiv$CC$_6$H$_4$C$\equiv$CC$\equiv$CC$_6$H$_4$C$\equiv$C) (**15**) have been prepared and their electrochemical (Ru complexes) and nonlinear optical properties assessed. Electronic communication between the metal centers in **10**, **11** and **15** diminishes as the π-delocalizable bridge is lengthened. Quadratic nonlinear optical (NLO) merit increases on replacing triarylphosphine by trialkylphosphine, the relative β values Au(4-C$\equiv$CC$_6$H$_4$NO$_2$)(PPh$_3$) < **1** < **3** being observed. Cubic NLO values are small for the gold complexes and much larger for the ruthenium examples. Complex **15** has the largest σ_2/MWt (two-photon absorption cross-section/molecular weight) value observed thus far for an organometallic complex. © 2002 Elsevier Science B.V. All rights reserved.

Keywords: Ruthenium; Gold; Hyperpolarizability; Acetylide; Electrochemistry; Nonlinear optics

1. Introduction

The nonlinear optical (NLO) properties of organometallic complexes have come under considerable scrutiny recently [2,3], alkynyl complexes in particular revealing large NLO responses. Gold acetylide complexes have good transparency characteristics ($\lambda_{max} < 350$ nm), and we have previously reported examples with significant β_{1064} and two-level corrected β_0 coefficients [4,5]; a summary of studies of the NLO properties of gold complexes has appeared recently in
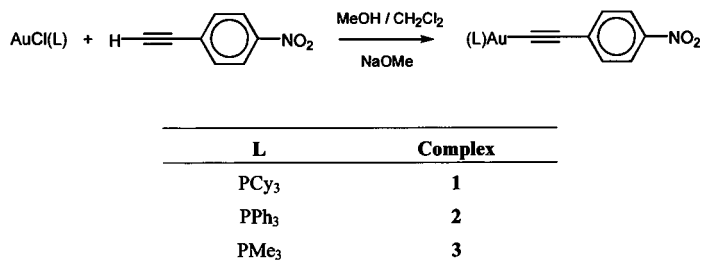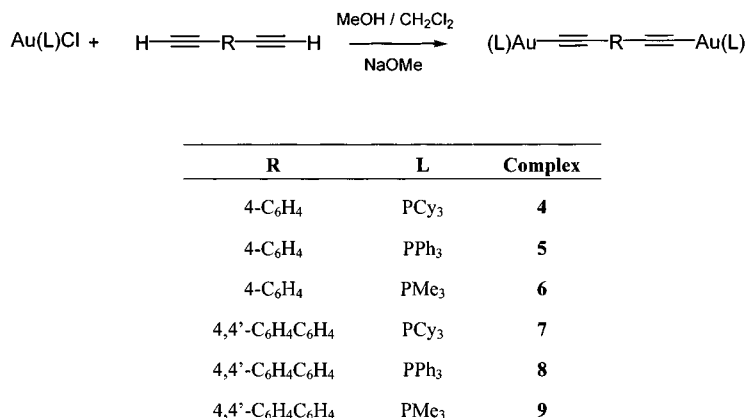
Ref. [6]. We report herein studies exploring the effect of phosphine variation on quadratic NLO merit in a system for which resonance-enhancement is minimal and, therefore, for which a realistic evaluation of this structural variation is possible.

The great majority of studies examining the NLO response of organometallics involve quadratic hyperpolarizabilities; the limited studies of cubic NLO merit have generally involved complexes with a donor–acceptor composition designed for enhanced quadratic response, and for which a 'cascade' effect to enhance the cubic NLO response is possible. Centrosymmetric compounds, for which all β components are zero, and for which a cascade effect is therefore not possible, are little explored. We also report herein studies of a range of centrosymmetric gold and ruthenium complexes, which,

---

[☆] Part 24: see Ref. [1].
* Corresponding author. Tel.: + 61-2-6125-2927; fax: + 61-2-6125-0760.
E-mail address: mark.humphrey@anu.edu.au (M.G. Humphrey).

Scheme 1. Syntheses of 4-nitrophenylalkynylgold complexes **1**–**3**.

R	L	Complex
4-C$_6$H$_4$	PCy$_3$	**4**
4-C$_6$H$_4$	PPh$_3$	**5**
4-C$_6$H$_4$	PMe$_3$	**6**
4,4'-C$_6$H$_4$C$_6$H$_4$	PCy$_3$	**7**
4,4'-C$_6$H$_4$C$_6$H$_4$	PPh$_3$	**8**
4,4'-C$_6$H$_4$C$_6$H$_4$	PMe$_3$	**9**

Scheme 2. Syntheses of alkynylbis{(phosphine)gold} complexes **4**–**9**.

for the latter, have resulted in complexes with extremely large cubic NLO coefficients for organometallics. The two-photon absorption (TPA) characteristics of quadrupolar compounds have recently commanded attention [7]; the present work also reports the first TPA data for quadrupolar organometallic complexes.

2. Results and discussion

2.1. Synthesis and characterization of σ-acetylide complexes

The synthetic methodologies employed for the preparation of the new complexes are adaptations of those successfully utilized for the preparation of the corresponding phenylacetylide complexes. Gold nitrophenylacetylides **1** and **3** and gold phosphine complexes **4**, **5**, **7** and **8**, which are binuclear complexes linked by 4-C≡CC$_6$H$_4$C≡C and 4,4'-C≡CC$_6$H$_4$C$_6$H$_4$C≡C ligands, were prepared in good yield by extending the method of Naulty et al. [5] (Schemes 1 and 2); complexes **6** and **9** have been reported recently by Puddephatt and co-workers [8], while complex **2** was reported by us previously [4]. The (tricyclohexylphosphine)gold complexes are significantly more soluble in common organic solvents than their (triphenylphosphine)gold analogs, an important factor when evaluating nonlinearities. The

bis{bis(diphenylphosphino)methane}ruthenium complex **11** was prepared by extending the method of Touchard et al. [9] (Scheme 3); complex **10** has been reported previously by Lewis and co-workers [10].

The centrosymmetric bis{bis(diphenylphosphino)-ethane}ruthenium complex **15** was prepared according to Scheme 4. Reaction of two equivalents of 4-HC≡CC$_6$H$_4$I with cis-[RuCl$_2$(dppe)$_2$] afforded trans-

R	Complex
4-C$_6$H$_4$	**10**
4,4'-C$_6$H$_4$C$_6$H$_4$	**11**
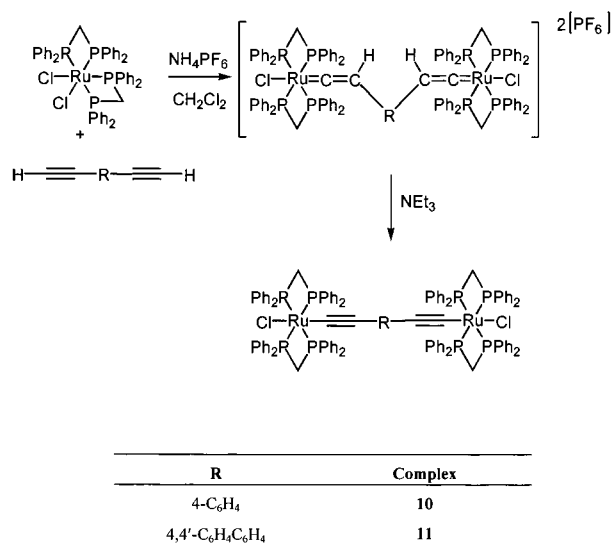
Scheme 3. Syntheses of alkynyl bis[bis{bis(diphenylphosphino)-methane}chlororuthenium] complexes **10** and **11**.
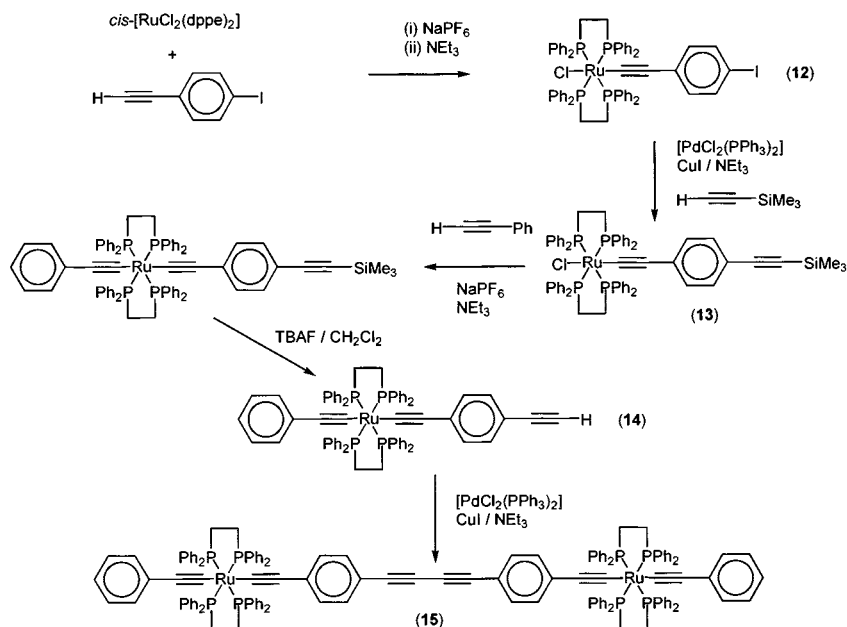
Scheme 4. Syntheses of complexes **12**–**15**.

Table 1
Cyclic voltammetric data for ruthenium complexes **10**, **11** and **15** [a]

Complex	$E_{1/2}$ Ru(II)/(III) (V)	$\Delta E_{1/2}$ (V)	$[i_{pc}/i_{pa}]$	K_{com}	Reference
trans,trans-[RuCl(dppm)$_2$(μ-4,4′-C≡CC$_6$H$_4$C≡C)RuCl(dppm)$_2$] (**10**)	0.22, 0.54	0.32	1.0, 1.0	2.6×10^5	This work
	0.26, 0.56	0.30	1.0, 1.0	1.2×10^5	[10]
trans,trans-[RuCl(dppm)$_2$(μ-4,4′-C≡CC$_6$H$_4$C$_6$H$_4$C≡C)RuCl(dppm)$_2$] (**11**)	0.41, 0.51	0.10	1.0, 1.0	4.9×10	This work
{trans-[Ru(C≡CPh)(dppe)$_2$]}$_2$(μ-4,4′-C≡CC$_6$H$_4$C≡CC≡CC$_6$H$_4$C≡C) (**15**)	0.58	0	1.0	0	This work

[a] Ferrocene/ferrocenium couple (0.56 V) as an internal standard.

[Ru(4-C≡CC$_6$H$_4$I)Cl(dppe)$_2$] (**12**) after basic work-up. The iodo substituent is amenable to Sonogashira coupling; thus, the reaction of **12** with trimethylsilylacetylene in the presence of Pd(II) and Cu(I) catalysts afforded trans-[Ru(4-C≡CC$_6$H$_4$C≡CSiMe$_3$)Cl(dppe)$_2$] (**13**). The reaction of **13** with phenylacetylene in the presence of triethylamine gave trans-[Ru(4-C≡CC$_6$-H$_4$C≡CSiMe$_3$)(C≡CPh)(dppe)$_2$], subsequent removal of the trimethylsilyl protecting group with fluoride affording trans-[Ru(4-C≡CC$_6$H$_4$C≡CH)(C≡CPh)(dppe)$_2$] (**14**). Finally, oxidative coupling of **14** utilizing Pd(II)/Cu(I) as catalysts gave {trans-[Ru(C≡CPh)(dppe)$_2$]}$_2$(μ-4,4′-C≡CC$_6$H$_4$C≡CC≡CC$_6$H$_4$C≡C) (**15**).

The new complexes were characterized by SI mass spectrometry, satisfactory microanalyses, UV–vis, IR, ^{1}H- and ^{31}P-NMR spectroscopy. Mass spectra for the gold complexes contain weak or nonexistent molecular ion signals, (phosphine)gold units being the most abundant ions observed. With the exception of **15**, all ruthenium complexes gave mass spectra with molecular ions or protonated molecular ions. UV–vis spectra contain bands in the range of 325–342 nm (gold complexes) and 340–370 nm (ruthenium complexes), and the IR spectra show characteristic coordinated ν(C≡C) bands in the range of 2106–2115 cm^{-1} (gold complexes) and 2057–2077 cm^{-1} (ruthenium complexes), the spectrum of **13** also showing a free ν(C≡C) band at 2148 cm^{-1}. ^{31}P-NMR spectra of all complexes contain one singlet resonance, consistent with the trans geometry at the ruthenium center and centrosymmetry in the binuclear complexes.

2.2. Electrochemical studies

The electrochemical data for the binuclear ruthenium complexes **10**, **11** and **15** are given in Table 1. Complex **10** was examined earlier by cyclic voltammetry [10]; the data are also included in Table 1, and are experimentally similar to data collected under our own experimental conditions. This series of complexes is of interest as it corresponds to a range of potentially π-delocalizable bridging units coupling the two

$Ru(L_2)_2X$ groups (L_2 = dppm, dppe; X = Cl, C≡CPh). All Ru(II)/(III) couples listed in Table 1 are essentially reversible, so an assessment of the electronic communication by considering the difference in Ru(II)/(III) couples ($\Delta E_{1/2}$) is appropriate. We have noted previously that *trans*-disposed phenylalkynyl ligands behave electronically as pseudo-halides in complexes of this type [11,12], so the progression in $\Delta E_{1/2}$ data should reflect changes in the nature of the bridging unit. Several studies assessing electronic communication between metal centers in binuclear acetylide complexes have been reported recently [10,13–16]; the present data affords the possibility of assessing the effect of bridge lengthening on electronic communication. Extending the length of the π-delocalizable bridge in proceeding from **10** to **11** and then **15** results in a decrease in electronic communication, as assessed by $\Delta E_{1/2}$. The comproportionation constants K_{com} for these complexes have been calculated and are listed in Table 1. Following the Robin and Day classification [17], **15** is a Class I binuclear complex, in which the metal centers are not interacting, **11** is a borderline Class I/Class II example, and **10** belongs to Class II, in which metal centers are weakly interacting.

2.3. Quadratic hyperpolarizabilities

We have determined the molecular quadratic nonlinearities of **1** and **3**, using hyper-Rayleigh scattering at 1064 nm; the results of these studies, β_{exp}, are given in Table 2, together with the two-level-corrected values β_0, and the corresponding data for relevant complexes. We have discussed previously the potential inadequacies of the two-state model [18]. The low-energy band for these complexes is MLCT in character; higher-energy bands involve transitions with other ligands, which result in little change in the dipole moment between ground and excited states, and hence little contribution to nonlinearity; therefore it is probable that the two-level-corrected values have some significance as an indicator of zero-frequency nonlinearity.

Introduction of acceptor nitro substituent in proceeding from [Au(C≡CPh)(PMe₃)] to **3** leads to the expected red-shift in λ_{max} and a significant increase in the quadratic optical nonlinearity. Replacing the triarylphosphine with trialkylphosphines in progressing from **2** to **1** and **3** results in an increase in nonlinearity, a result that contrasts with our earlier observation of a similar ligand replacement in nitropyridylalkynyl complexes. Trialkylphosphines are stronger donors than triarylphosphines, whereas the latter provide additional π-delocalization possibilities, and the relative importance of these two factors for quadratic NLO merit appears to vary in proceeding from phenylalkynyl to pyridylalkynyl complexes.

2.4. Cubic hyperpolarizabilities

Third-order nonlinearities for **1–4**, **7**, **10**, **11** and **15** were determined by *Z*-scan at 800 nm, data being collected in Table 3; complexes **5**, **6**, **8**, and **9** were insufficiently soluble in CH_2Cl_2 or THF to acquire useful data. An electronic origin for cubic nonlinearities in related metal acetylide complexes has been demonstrated previously by degenerate four-wave mixing measurements [19], and nonlinearities for the present series of compounds are therefore likely to be electronic in origin.

The effect on refractive nonlinearity γ_{real} of phosphine ligand replacement in the dipolar series **1–3** is negligible, all γ_{real} data being equivalent within the error margins; unlike **2**, no detectable γ_{imag} component is present for **1** and **3**. The binuclear gold complexes **4** and **7** have very small cubic nonlinearities. Molecular second hyperpolarizabilities for the binuclear ruthenium complexes **10**, **11** and **15** are significantly larger; thus, replacing $Au(PCy_3)$ with *trans*-RuCl(dppm)₂ in proceeding from **4** to **10** or **7** to **11** results in a dramatic increase in $|\gamma|$. For the ruthenium complexes, negative γ_{real} and significant γ_{imag} components are consistent with the presence of two-photon states contributing to the observed nonlinearity. The present data for centrosymmetric complexes complement our previously re-

Table 2
Experimental linear optical spectroscopic and quadratic nonlinear optical response parameters [a]

Compound	λ_{max} (nm) [ε (10^4 M^{-1} cm^{-1})]	β_{exp} (10^{-30} esu) [b]	β_0 (10^{-30} esu)	Reference
[Au(4-C≡CC₆H₄NO₂)(PCy₃)] (**1**)	342 [2.2]	31	16	This work
[Au(4-C≡CC₆H₄NO₂)(PPh₃)] (**2**)	338 [2.5]	22	12	[4]
[Au(4-C≡CC₆H₄NO₂)(PMe₃)] (**3**)	339 [1.3]	50	27	This work
[Au(C≡CPh)(PMe₃)]	296 [1.3]	6	4	[4]
[Au(C≡CC₅H₃N-2-NO₂-5)(PPh₃)]	339 [2.6]	38	20	[5]
[Au(C≡CC₅H₃N-2-NO₂-5)(PMe₃)]	340 [1.6]	12	6	[5]

[a] All measurements in THF solvent. All complexes are optically transparent at 1064 nm; values ± 10%.
[b] HRS at 1064 nm corrected for resonance enhancement at 532 nm using the two-level model with $\beta_0 = \beta[1-(2\lambda_{max}/1064)^2][1-(\lambda_{max}/1064)^2]$; damping factors not included.

Table 3
Experimental linear optical spectroscopic and cubic nonlinear optical response parameters [a]

Compound	λ_{max} (nm) [ε (10^4 M^{-1} cm^{-1})]	γ_{real} (10^{-36} esu)	γ_{imag} (10^{-36} esu)	$|\gamma|$ (10^{-36} esu)	Reference
[Au(4-C≡CC₆H₄NO₂)(Pcy₃)] (**1**)	342 [2.2]	100 ± 50	–	100 ± 50	This work
[Au(4-C≡CC₆H₄NO₂)(PPh₃)] (**2**)	338 [2.5]	120 ± 40	20 ± 15	120 ± 40	This work
[Au(4-C≡CC₆H₄NO₂)(Pme₃)] (**3**)	339 [1.3]	150 ± 50	–	150 ± 50	This work
[(PCy₃)Au-4-C≡CC₆H₄C≡CAu(PCy₃)] (**4**)	325 [5.6]	≤ 250	–	≤ 250	This work
[(PCy₃)Au-4,4′-C≡CC₆H₄C₆H₄C≡CAu(PCy₃)] (**7**)	324 [6.5]	-300 ± 200	0 ± 30	300 ± 200	This work
trans,trans-[RuCl(dppm)₂(μ-4,4′-C≡CC₆H₄C≡C)-RuCl(dppm)₂] (**10**)	354 [4.2]	-3200 ± 500	1400 ± 300	3500 ± 600	This work
trans,trans-[RuCl(dppm)₂(μ-4,4′-C≡CC₆H₄-C₆H₄C≡C)RuCl(dppm)₂] (**11**)	360 [9.0]	-1100 ± 300	300 ± 60	1100 ± 300	This work
trans-[RuCl(4-C≡CC₆H₄NO₂)(dppm)₂]	466 [1.6]	170 ± 30	230 ± 50	290 ± 60	[33]
trans-[RuCl(4,4′-C≡CC₆H₄C₆H₄NO₂)(dppm)₂]	448 [1.8]	140 ± 30	64 ± 10	150 ± 30	[33]
{*trans*-[Ru(C≡CPh)(dppe)]}₂(μ-4,4′-C≡CC₆H₄-C≡CC≡CC₆H₄C≡C) (**15**)	438 [6.8]	-4000 ± 1500	$12\,000 \pm 2000$	$13\,000 \pm 2400$	This work

[a] All measurements as THF solutions (all complexes are optically transparent at 800 nm). All results are referenced to silica, nonlinear refractive index $n_2 = 3 \times 10^{-16}$ cm² W^{-1}.

ported data for dipolar complexes; replacing NO_2 in the dipolar examples with *trans*-[(C≡C)RuCl(dppm)₂] to afford **10** or **11** results in significant increases in $|\gamma|$, the presence of the second electron-rich metal center being more important than the dipolar composition in enhancing cubic NLO merit. These data suggest that extending π-delocalization is the critical factor, consistent with the experience with organic compounds. Significant extension of the π-system, in proceeding from **10**, **11** to **15**, results in a further considerable increase in $|\gamma|$. Complex **15** has a very large γ_{imag} component. We have reported earlier two-photon absorption cross-sections at 800 nm for a first-generation alkynylruthenium dendrimer and its components [20]. Evaluating the TPA cross-section σ_2 for **15** (2910×10^{-50} cm⁴ s) reveals that it is similar in magnitude to that of the dendrimer (4800×10^{-50} cm⁴ s); the σ_2/MWt is considerably larger for **15** (1.3×10^{-50} cm⁴ s mol g⁻¹) than for the dendrimer (0.47×10^{-50} cm⁴ s mol g⁻¹), and indeed is the largest thus far for an organometallic complex.

3. Conclusions

The present studies have afforded a number of results. Nonlinearities for the dipolar gold complexes are low compared with the related ruthenium complexes reported earlier [5,18,21,22], although they have enhanced optical transparency; co-ligand replacement does not have a clear-cut effect on quadratic nonlinearity. Binuclear gold complexes have diminished solubility, which can be improved sufficiently to afford cubic NLO data by employing PCy₃; $|\gamma|$ values for these digold complexes are uniformly low. Linked ruthenium complexes can exhibit electronic communication, as

assessed by cyclic voltammetry, the extent of which diminishes as the π-bridge is lengthened. Cubic NLO responses for the diruthenium complexes are large, with evidence for two-photon effects contributing to the observed responses at 800 nm. The $|\gamma|$ value for **15** is very large, and its molecular weight-scaled two-photon absorption cross-section is the largest reported thus far for an organometallic complex, suggesting that similar compounds may have potential in TPA applications.

4. Experimental

4.1. General conditions, reagents and instruments

All reactions were performed under a nitrogen atmosphere with the use of standard Schlenk techniques unless otherwise stated. Dichloromethane and Et₃N were dried by distilling over CaH₂, Et₂O and THF were dried by distilling over sodium/benzophenone, and other solvents were used as received. 'Petroleum spirit' refers to a fraction of petroleum ether of boiling range 60–80 °C. Chromatography was carried out in silica gel (230–400 mesh ASTM) or basic ungraded alumina. The following reagents were prepared by the literature procedures: [AuCl(PPh₃)] [23], [AuCl(PMe₃)] [24], [AuCl(PCy₃)] [25], 4-HC≡CC₆H₄C≡CH, 4,4′-HC≡CC₆H₄C₆H₄C≡CH and 4-HC≡CC₆H₄NO₂ [26], 4-IC₆H₄C≡CSiMe₃ and 4-IC₆H₄C≡CH [27], *cis*-[RuCl₂(dppm)₂] and *cis*-[RuCl₂(dppe)₂] [28]. Ferrocene (Aldrich), Me₃SiC≡CH (Aldrich), PhC≡CH (Aldrich), [PdCl₂(PPh₃)₂] (PMO), CuI (Aldrich), NH₄PF₆ (Aldrich), NaPF₆ (Aldrich), tetramethylethylenediamine (TMEDA) (Aldrich), tetra-*n*-butylammonium fluoride (Aldrich), *t*-butyllithium (Aldrich) and 4-IC₆H₄CHO (Karl Industries) were used as received.

EI (electron impact) mass spectra [both unit resolution and high resolution (HR)] were recorded using a VG Autospec instrument (70 eV electron energy, 8 kV accelerating potential) and secondary ion mass spectra (SIMS) were recorded using a VG ZAB 2SEQ instrument (30 kV Cs$^+$ ions, current 1 mA, accelerating potential 8 kV, 3-nitrobenzyl alcohol matrix) at the Research School of Chemistry, Australian National University; peaks are reported as m/z (assignment, relative intensity). Microanalyses were carried out at the Research School of Chemistry, Australian National University. Infrared spectra were recorded either as 1% KBr discs or CH$_2$Cl$_2$ solutions using a Perkin–Elmer System 2000 FTIR. ^{1}H- and ^{31}P-NMR spectra were recorded using a Varian Gemini-300 FT NMR spectrometer and are referenced to residual CHCl$_3$ (7.24 ppm), d-CHCl$_3$ (77.0 ppm) or external 85% H$_3$PO$_4$ (0.0 ppm), respectively. The assignments follow the numbering scheme shown in Fig. 1. UV–vis spectra of solutions were recorded in THF in 1 cm quartz cells using a Cary 4 spectrophotometer. Electrochemical measurements were recorded using a MacLab 400 interface and MacLab potentiostat from ADInstruments. The supporting electrolyte was 0.1 M (N^{n}Bu$_4$)PF$_6$ in distilled, deoxygenated CH$_2$Cl$_2$. Solutions containing ca. 1×10^{-3} M complex were maintained under Ar. Measurements were carried out at room temperature (r.t.) using platinum disc working-, Pt wire auxiliary- and Ag/AgCl reference-electrodes, such that the ferrocene/ferrocenium redox couple was located at 0.56 V (peak separation around 0.09 V). Scan rates were typically 100 mV s^{-1}.

4.2. Syntheses of metal complexes

4.2.1. [Au(4-C≡CC$_6$H$_4$NO$_2$)(PCy$_3$)] (1)

[AuCl(PCy$_3$)] (200 mg, 0.39 mmol), 4-HC≡CC$_6$H$_4$-NO$_2$ (69 mg, 0.47 mmol) and CuI (5 mg) were stirred in a solution of CH$_3$ONa in MeOH (0.1 M, 15 ml) for 12 h. Dichloromethane (100 ml) was added and the solution filtered through a plug of silica. The solvent was removed under vacuum; the material was then triturated under petroleum spirit to yield 201 mg (82%) of the pale-yellow product. Anal. Calc. for C$_{26}$H$_{37}$-AuNO$_2$P: C, 50.08; H, 5.98; N, 2.25. Found: C, 49.95; H, 6.15; N, 2.05%. IR (cm^{-1}, CH$_2$Cl$_2$): ν(C≡C) 2113. UV–vis: λ (nm) (ε, M^{-1} cm^{-1}) (THF): 342 (21 700). ^{1}H-NMR (CDCl$_3$, 300 MHz, δ ppm): 1.10–2.10 (m, 33H, Cy), 7.55 (d, 2H, J_{HH} = 9 Hz, H_4), 8.08 (d, 2H, J_{HH} = 9 Hz, H_5). ^{31}P-NMR (CDCl$_3$, 121 MHz, δ ppm): 56.8. SIMS; m/z: 1100 ([M + PCy$_3$]$^+$, 25), 624 ([M]$^+$, 50), 477 [Au(PCy$_3$)]$^+$, 100).

4.2.2. [Au(4-C≡CC$_6$H$_4$NO$_2$)(PMe$_3$)] (3)

[AuCl(PMe$_3$)] (180 mg, 0.58 mmol) and 4-HC≡CC$_6$H$_4$NO$_2$ (103 mg, 0.70 mmol) were stirred in a solution of CH$_3$ONa in MeOH (0.1 M, 15 ml) for 16 h. After this time, a solid yellow product precipitated which was collected by filtration. Yield 198 mg (81%). Anal. Calc. for C$_{11}$H$_{13}$AuNO$_2$P: C, 31.52; H, 3.13; N, 3.34. Found: C, 31.09; H, 3.21; N, 3.28%. IR (cm^{-1}, CH$_2$Cl$_2$): ν(C≡C) 2115. UV–vis: λ (nm) (ε, M^{-1} cm^{-1}) (THF): 339 (13 500). ^{1}H-NMR (CDCl$_3$, 300 MHz, δ ppm): 1.51 (m, 9H, Me), 7.52 (d, 2H, J_{HH} = 9 Hz, H_4), 8.08 (d, 2H, J_{HH} = 9 Hz, H_5). ^{31}P-NMR (CDCl$_3$, 121 MHz, δ ppm): 1.4. SIMS; m/z: 349 ([Au(PMe$_3$)$_2$]$^+$, 100), 273 ([Au(PMe$_3$)]$^+$, 25).
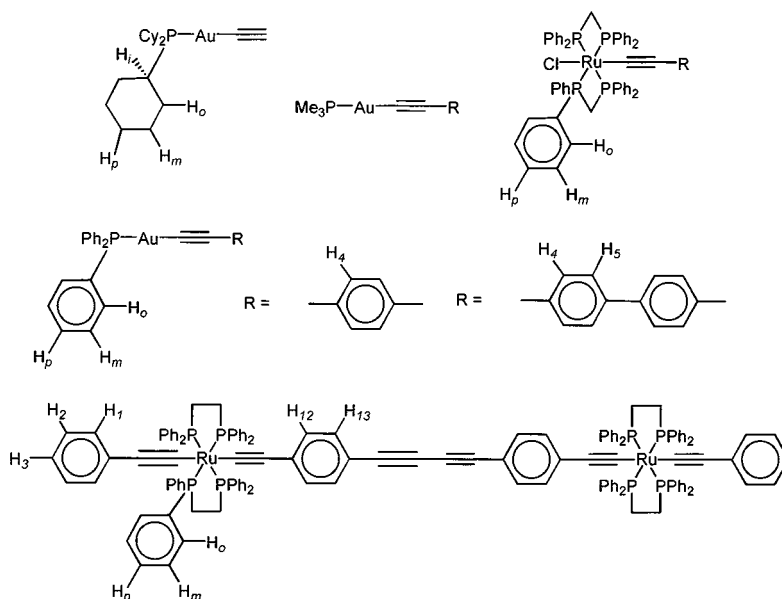
Fig. 1. Numbering scheme for NMR spectral assignments for **1**–**15**.

4.2.3. [(PCy₃)Au(μ-4-C≡CC₆H₄C≡C)Au(PCy₃)] (4)

[AuCl(PCy₃)] (200 mg, 0.39 mmol), 4-HC≡CC₆H₄C≡CH (24 mg, 0.19 mmol) and CuI (5 mg) were stirred in a solution of CH₃ONa in MeOH (0.1 M, 15 ml) for 12 h. Dichloromethane (100 ml) was added and the solution filtered through a plug of silica. The solvent was removed under vacuum to yield 183 mg (87%) of the pale-yellow product. Anal. Calc. for $C_{46}H_{70}Au_2P_2$: C, 51.21; H, 6.54. Found: C, 51.30; H, 6.45%. IR (cm⁻¹, CH₂Cl₂): ν(C≡C) 2115. UV–vis: λ (nm) (ε, M⁻¹ cm⁻¹) (THF): 325 (56 000), 306 (40 400). ¹H-NMR (CDCl₃, 300 MHz, δ ppm): 1.20–2.00 (m, 66H, Cy), 7.31 (s, 4H, C₆H₄). ³¹P-NMR (CDCl₃, 121 MHz, δ ppm): 56.8. SIMS; m/z: 1079 ([M]⁺, 15), 757 ([Au(PCy₃)₂]⁺, 100), 477 ([PCy₃]⁺, 100).

4.2.4. [(PPh₃)Au(μ-4-C≡CC₆H₄C≡C)Au(PPh₃)] (5)

[AuCl(PPh₃)] (230 mg, 0.46 mmol), 4-HC≡CC₆H₄-C≡CH (29 mg, 0.23 mmol) and CuI (5 mg) were stirred in a solution of CH₃ONa in MeOH (0.1 M, 15 ml) for 12 h. Dichloromethane (100 ml) was added and the solution filtered through a plug of silica. The solvent was removed under vacuum to yield 183 mg (87%) of the pale-yellow product. Anal. Calc. for $C_{46}H_{34}Au_2P_2$: C, 52.99; H, 3.29. Found: C, 52.46; H, 3.39%. IR (cm⁻¹, CH₂Cl₂): ν(C≡C) 2108. UV–vis: λ (nm) (ε, M⁻¹ cm⁻¹) (THF): 329 (53 800), 309 (37 700). ¹H-NMR (CDCl₃, 300 MHz, δ ppm): 7.36 (s, 4H, H_4, H_5), 7.40–7.60 (m, 30H, Ph). ³¹P-NMR (CDCl₃, 121 MHz, δ ppm): 42.8. SIMS; m/z: 1042 ([M]⁺, 5), 721 ([Au(PPh₃)₂]⁺, 10), 459 ([AuPPh₃]⁺, 65).

4.2.5. [(PCy₃)Au(μ-4,4'-C≡CC₆H₄C₆H₄C≡C)Au(PCy₃)] (7)

[AuCl(PCy₃)] (200 mg, 0.39 mmol), 4,4'-HC≡CC₆H₄-C₆H₄C≡CH (39 mg, 0.19 mmol) and CuI (5 mg, 0.03 mmol) were stirred in a solution of CH₃ONa in MeOH (0.1 M, 15 ml) for 16 h. The material was collected by filtration, washed with MeOH and then with petroleum spirit, affording 253 mg (56%) of the white product. Anal. Calc. for $C_{52}H_{74}Au_2P_2$: C, 54.07; H, 6.46%. Found: C, 53.33; H, 6.38%. IR (cm⁻¹, CH₂Cl₂): ν(C≡C) 2115. UV–vis: λ (nm) (ε, M⁻¹ cm⁻¹) (THF): 325 (56 000), 306 (40 400). ¹H-NMR (CDCl₃, 300 MHz, δ ppm): 1.20–2.00 (m, 66H, Cy), 7.31 (s, 4H, C₆H₄). ³¹P-NMR (CDCl₃, 121 MHz, δ ppm): 56.8. SIMS; m/z: 477 ([Au(PCy₃)₃]⁺, 100).

4.2.6. [(PPh₃)Au(μ-4,4'-C≡CC₆H₄C₆H₄C≡C)Au(PPh₃)] (8)

[AuCl(PPh₃)] (150 mg, 0.30 mmol), 4,4'-HC≡CC₆H₄-C₆H₄C≡CH (28 mg, 0.14 mmol) and CuI (5 mg) were stirred in a solution of CH₃ONa in MeOH (0.1 M, 15 ml) for 16 h. The material was collected by filtration, washed with MeOH and then with petroleum spirit, affording 118 mg (76%) of the white product. Anal.

Calc. for $C_{52}H_{38}Au_2P_2$: C, 55.83; H, 3.42%. Found: C, 54.87; H, 3.53%. IR (cm⁻¹, CH₂Cl₂): ν(C≡C) 2106. UV–vis: λ (nm) (ε, M⁻¹ cm⁻¹) (THF): 325 (65 600). ¹H-NMR (CDCl₃, 300 MHz, δ ppm): 7.35–7.60 (m, 38H, Ph + C₆H₄). ³¹P-NMR (CDCl₃, 121 MHz, δ ppm): 42.8. SIMS; m/z: 1119 ([M]⁺, 10), 757 ([Au(PPh₃)₂]⁺, 35), 459 ([Au(PPh₃)]⁺, 100).

4.2.7. trans,trans-[RuCl(dppm)₂(μ-4,4'-C≡CC₆H₄C₆H₄C≡C)RuCl(dppm)₂]·H₂O (11)

cis-[RuCl₂(dppm)₂] (200 mg, 0.22 mmol), 4,4'-HC≡CC₆H₄C₆H₄C≡CH (21 mg, 0.11 mmol) and NH₄PF₆ (69 mg, 0.42 mmol) were heated in refluxing CH₂Cl₂ (25 ml) for 9 h. The solution was filtered and the solvent removed from the filtrate under reduced pressure. The residue was triturated with Et₂O and the resultant solid was then redissolved in CH₂Cl₂. Triethylamine (1 ml) was added with stirring and the solution eluted through an alumina plug with CH₂Cl₂. Removal of the solvent under reduced pressure yielded 145 mg (68%) of the yellow product. Anal. Calc. for $C_{116}H_{98}OP_8Ru_2$: C, 68.67; H, 4.87%. Found: C, 67.85; H, 5.04%. IR (cm⁻¹, CH₂Cl₂): ν(C≡C) 2077. UV–vis: λ (nm) (ε, M⁻¹ cm⁻¹) (THF): 360 (90 400). ¹H-NMR (CDCl₃, 300 MHz, δ ppm): 1.55 (s, 2H, H₂O), 4.90 (m, 8H, PCH₂P), 6.10 (m, 4H, H_4), 7.00–7.60 (m, 84H, Ph + H_5). ³¹P-NMR (CDCl₃, 121 MHz, δ ppm): −5.9. SIMS; m/z: 2012 ([M + 2H]⁺, 5), 905 ([RuCl(dppm)₂]⁺, 85), 870 ([Ru(dppm)₂]⁺, 100).

4.2.8. trans-[Ru(4-C≡CC₆H₄I)Cl(dppe)₂] (12)

cis-[RuCl₂(dppe)₂] (500 mg, 0.52 mmol), 4-HC≡CC₆H₄I (240 mg, 1.05 mmol) and sodium hexafluorophosphate (200 mg, 1.19 mmol) were stirred in CH₂Cl₂ (20 ml) for 6 h at r.t. Petroleum spirit (30 ml, deoxygenated) was added via cannula and the total solvent volume reduced to ∼25 ml in vacuo. The mixture was filtered using Schlenk techniques and the residue dissolved in CH₂Cl₂ (20 ml). Sodium methoxide (65 mg, 1.19 mmol, in 2 ml of MeOH) was added to deprotonate the vinylidene complex formed. The solvent was removed in vacuo and the residue purified by column chromatography, eluting with 4:1 CH₂Cl₂–petroleum spirit. The product was precipitated by removing the CH₂Cl₂ on a rotary evaporator. Upon filtering, 480 mg of the yellow powder was isolated (80%). Anal. Calc. for $C_{60}H_{52}ClIP_4Ru$: C, 62.10; H, 4.52. Found: C, 62.34; H, 4.30%. UV–vis: λ (nm) (ε, M⁻¹ cm⁻¹) (THF): 340 (24 500). IR (cm⁻¹, CH₂Cl₂): ν(C≡C) 2068. ¹H-NMR (CDCl₃, 300 MHz, δ ppm): 2.63 (m, 8H, CH₂), 6.30 (d, J_{HH} = 8 Hz, 2H, H_{13}), 6.90–7.44 (42H, Ph + H_{12}). ³¹P-NMR (CDCl₃, 121 MHz, δ ppm): 50.1. SIMS; m/z: 1160 ([M]⁺, 17), 1125 ([M − Cl]⁺, 32), 897 ([Ru(dppe)₂]⁺, 23), 499 ([Ru(dppe)]⁺, 16).

4.2.9. trans-[Ru(4-C≡CC₆H₄C≡CSiMe₃)Cl(dppe)₂] (13)

trans-[Ru(4-C≡CC₆H₄I)Cl(dppe)₂] (12) (500 mg, 0.43 mmol) and trimethylsilylacetylene (180 ml, 1.27 mmol) were dissolved in THF (15 ml). Dichlorobis(triphenylphosphine)palladium(II) (10 mg, 0.014 mmol), CuI (10 mg, 0.052 mmol) and Et₃N (2 ml) were added with stirring. The mixture was stirred for 20 min at r.t. The solvent was then removed in vacuo and the residue dissolved in CH₂Cl₂ and passed through an alumina plug, eluting with CH₂Cl₂. Petroleum spirit was added (∼ 50 ml) and the solvent removed using a rotary evaporator, affording 300 mg (62%) of the product as a yellow powder. Anal. Calc. for $C_{65}H_{61}ClP_4RuSi$: C, 69.05; H, 5.44. Found: C, 68.51; H, 5.50%. UV–vis: λ (nm) (ε, M^{-1} cm^{-1}) (THF): 370 (33 100). IR (cm^{-1}, CH₂Cl₂): ν(C≡C) 2148, 2065. ¹H-NMR (CDCl₃, 300 MHz, δ ppm): 0.24 (s, 9H, Me), 2.66 (m, 8H, CH₂), 6.46 (d, J_{HH} = 8 Hz, 2H, H₁₃), 6.87–7.40 (42H, Ph + H₁₂). ³¹P-NMR (CDCl₃, 121 MHz, δ ppm): 49.8. SIMS; m/z: 1130 ([M]⁺, 100), 1095 ([M − Cl]⁺, 20), 897 ([Ru(dppe)₂ − H]⁺, 25), 499 ([Ru(dppe) − H]⁺, 25).

4.2.10. trans-[Ru(4-C≡CC₆H₄C≡CH)(C≡CPh)(dppe)₂] (14)

trans-[Ru(4-C≡CC₆H₄C≡CSiMe₃)Cl(dppe)₂] (13) (720 mg, 0.64 mmol), phenylacetylene (140 µl, 1.28 mmol), sodium hexafluorophosphate (220 mg, 1.31 mmol) and Et₃N were stirred in CH₂Cl₂ for 4 h at r.t. The solvent was then removed in vacuo and the residue purified by column chromatography, eluting first with petroleum spirit to remove excess acetylene, and then with 4:1 CH₂Cl₂–petroleum spirit to remove the yellow complex. The solvent was removed, and the material was then dissolved in CH₂Cl₂ (20 ml) and tetra-n-butylammonium fluoride (0.40 ml, 1 M solution in THF) was added with stirring. The mixture was stirred for 30 min at r.t. The solvent was then removed in vacuo and the residue purified by column chromatography in alumina, eluting with 2:3 CH₂Cl₂–petroleum spirit. The solvent was removed using a rotary evaporator and 335 mg (54%) of the yellow powder was collected. Anal. Calc. for $C_{70}H_{58}P_4Ru$: C, 74.79; H, 5.20. Found: C, 74.48; H, 5.20%. UV–vis: λ (nm) (ε, M^{-1} cm^{-1}) (THF): 361 (35 400). IR (cm^{-1}, CH₂Cl₂): ν(C≡C) 2057, ν(C≡CH) 3294. ¹H-NMR (CDCl₃, 300 MHz, δ ppm): 2.60 (m, 8H, CH₂), 3.09 (s, 1H, C≡CH), 6.58 (d, J_{HH} = 8 Hz, 2H, H₁₂ or H₁₃), 6.79 (d, J_{HH} = 8 Hz, 2H, H₁₂ or H₁₃), 6.89–7.59 (45H, Ph). ³¹P-NMR (CDCl₃, 121 MHz, δ ppm): 54.5. SIMS; m/z: 1160 ([M]⁺, 17).

4.2.11. {trans-[Ru(C≡CPh)(dppe)₂]}₂(µ-4,4'-C≡CC₆H₄C≡CC≡CC₆H₄C≡C)·2(H₂O) (15)

trans-[Ru(4-C≡CC₆H₄C≡CH)(C≡CPh)(dppe)₂] (14) (180 mg, 0.16 mmol) was dissolved in CH₂Cl₂ (20 ml) and PdCl₂(PPh₃)₂ (8 mg) and CuI (4 mg) were added with stirring. The solution was stirred for 6 h and then passed through an alumina plug. The solvent was removed using a rotary evaporator and 54 mg (30%) of the yellow powder was collected. Anal. Calc. for $C_{140}H_{118}P_8O_2Ru_2$: C, 73.67; H, 5.21. Found: C, 73.20; H, 5.47%. UV–vis: λ (nm) (ε, M^{-1} cm^{-1}) (THF): 438 (67 700). IR (cm^{-1}, CH₂Cl₂): ν(C≡C) 2058. ¹H-NMR (CDCl₃, 300 MHz, δ ppm): 2.62 (m, 16H, CH₂), 6.40–7.60 (98H, Ph + H₁ + H₁₂ + H₁₃). ³¹P-NMR (CDCl₃, 121 MHz, δ ppm): 54.4. SIMS; m/z: 999 ([Ru(C≡CPh)(dppe)₂]⁺, 10), 898 ([Ru(dppe)₂]⁺, 75).

4.3. Hyper-Rayleigh scattering measurements

An injection-seeded Nd:YAG laser (Q-switched Nd:YAG Quanta Ray GCR5, 1064 nm, 8 ns pulses, 10 Hz) was focused into a cylindrical cell (7 ml) containing the sample. The intensity of the incident beam was varied by rotation of a half-wave plate placed between crossed polarizers. Part of the laser pulse was sampled by a photodiode to measure the vertically polarized incident light intensity. The frequency doubled light was collected by an efficient condenser system and detected by a photomultiplier. The harmonic scattering and linear scattering were distinguished by appropriate filters; gated integrators were used to obtain intensities of the incident and harmonic scattered light. The absence of a luminescence contribution to the harmonic signal was confirmed by using interference filters at different wavelengths near 532 nm. All measurements were performed in THF using p-nitroaniline (β = 21.4×10^{-30} esu) [29] as a reference. Solutions were sufficiently dilute such that the absorption of scattered light was negligible. Further details on the experimental procedure are reported in Refs. [30,31].

4.4. Z-scan measurements

Measurements were performed at 800 nm using a system consisting of a Coherent Mira Ar-pumped Ti-sapphire laser generating a mode-locked train of ca. 100 fs pulses and a home-built Ti-sapphire regenerative amplifier pumped with a frequency-doubled Q-switched pulsed YAG laser (Spectra Physics GCR) at 30 Hz and employing chirped pulse amplification. THF solutions were examined in a glass cell with a 0.1 cm path length. The Z-scans were recorded at two concentrations for each compound and the real and imaginary part of the nonlinear phase change determined by numerical fitting [32]. The real and imaginary parts of the hyperpolarizability of the solute were then calculated by assuming linear concentration dependencies of the solution susceptibility. The nonlinearities and light intensities were calibrated using measurements of a 1 mm thick silica plate for which the nonlinear refractive index $n_2 = 3 \times 10^{-16}$ cm^2 W^{-1} was assumed.

Acknowledgements

References

[1] M.P. Cifuentes, C.E. Powell, M.G. Humphrey, G.A. Heath, M. Samoc, B. Luther-Davies, J. Phys. Chem. A 105 (2001) 9625.

[2] I.R. Whittall, A.M. McDonagh, M.G. Humphrey, M. Samoc, Adv. Organomet. Chem. 43 (1999) 349.

[3] I.R. Whittall, A.M. McDonagh, M.G. Humphrey, M. Samoc, Adv. Organomet. Chem. 42 (1998) 291.

[4] I.R. Whittall, M.G. Humphrey, S. Houbrechts, A. Persoons, D.C.R. Hockless, Organometallics 15 (1996) 5738.

[5] R.H. Naulty, M.P. Cifuentes, M.G. Humphrey, S. Houbrechts, C. Boutton, A. Persoons, G.A. Heath, D.C.R. Hockless, B. Luther-Davies, M. Samoc, J. Chem. Soc. Dalton Trans. (1997) 4167.

[6] M.G. Humphrey, Gold Bull. 33 (2000) 97.

[7] M. Albota, D. Beljonne, J.L. Bredas, J.E. Ehrlich, J.Y. Fu, A.A. Heikal, S.E. Hess, T. Kogej, M.D. Levin, S.R. Marder, D. McCord-Maughon, J.W. Perry, H. Rockel, M. Rumi, C. Subramaniam, W.W. Webb, X.L. Wu, C. Xu, Science 281 (1998) 1653.

[8] G.C. Jia, R.J. Puddephatt, J.D. Scott, J.J. Vittal, Organometallics 12 (1993) 3565.

[9] D. Touchard, P. Haquette, N. Pirio, L. Toupet, P.H. Dixneuf, Organometallics 12 (1993) 3132.

[10] M.C.B. Colbert, J. Lewis, N.J. Long, P.R. Raithby, M. Younus, A.J.P. White, D.J. Williams, N.N. Payne, L. Yellowlees, D. Beljonne, N. Chawdhury, R.H. Friend, Organometallics 17 (1998) 3034.

[11] J.E. McGrady, T. Lovell, R. Stranger, M.G. Humphrey, Organometallics 16 (1997) 4004.

[12] A.M. McDonagh, M.G. Humphrey, M. Samoc, B. Luther-Davies, S. Houbrechts, T. Wada, H. Sasabe, A. Persoons, J. Am. Chem. Soc. 121 (1999) 1405.

[13] C. Lebreton, D. Touchard, L. Le Pichon, A. Daridor, L. Toupet, P.H. Dixneuf, Inorg. Chim. Acta 272 (1998) 188.

[14] O. Lavastre, J. Plass, P. Bachmann, S. Guesmi, C. Moinet, P.H. Dixneuf, Organometallics 16 (1997) 184.

[15] N.D. Jones, M.O. Wolf, D.M. Giaquinta, Organometallics 16 (1997) 1352.

[16] Y.B. Zhu, O. Clot, M.O. Wolf, G.P.A. Yap, J. Am. Chem. Soc. 120 (1998) 1812.

[17] P. Zanello, S. Tamburini, P.A. Vigato, G.A. Mazzocchin, Coord. Chem. Rev. 77 (1987) 165.

[18] I.R. Whittall, M.P. Cifuentes, M.G. Humphrey, B. Luther-Davies, M. Samoc, S. Houbrechts, A. Persoons, G.A. Heath, D.C.R. Hockless, J. Organomet. Chem. 549 (1997) 127.

[19] I.R. Whittall, M.G. Humphrey, M. Samoc, J. Swiatkiewicz, B. Luther-Davies, Organometallics 14 (1995) 5493.

[20] A.M. McDonagh, M.G. Humphrey, M. Samoc, B. Luther-Davies, Organometallics 18 (1999) 5195.

[21] I.R. Whittall, M.G. Humphrey, A. Persoons, S. Houbrechts, Organometallics 15 (1996) 1935.

[22] R.H. Naulty, A.M. McDonagh, I.R. Whittall, M.P. Cifuentes, M.G. Humphrey, S. Houbrechts, J. Maes, A. Persoons, G.A. Heath, D.C.R. Hockless, J. Organomet. Chem. 563 (1998) 137.

[23] C.A. McAuliffe, R.V. Parish, P.D. Randall, J. Chem. Soc. Dalton Trans. (1979) 1730.

[24] M.I. Bruce, E. Horn, J.G. Matisons, M.R. Snow, Aust. J. Chem. 37 (1984) 1163.

[25] J. Bailey, J. Inorg. Nucl. Chem. 35 (1973) 1921.

[26] S. Takahashi, Y. Kuroyama, K. Sonogashira, N. Hagihara, Synthesis (1980) 627.

[27] R.P. Hsung, C.E.D. Chidsey, L.R. Sita, Organometallics 14 (1995) 4808.

[28] B. Chaudret, G. Commenges, R. Poilblanc, J. Chem. Soc. Dalton Trans. (1984) 1635.

[29] M. Stahelin, D.M. Burland, J.E. Rice, Chem. Phys. Lett. 191 (1992) 245.

[30] K. Clays, A. Persoons, Rev. Sci. Instrum. 63 (1992) 3285.

[31] S. Houbrechts, K. Clays, A. Persoons, Z. Pikramenou, J.-M. Lehn, Chem. Phys. Lett. 258 (1996) 485.

[32] M. Sheik-bahae, A.A. Said, T. Wei, D.J. Hagan, E.W. van-Stryland, IEEE J. Quantum Electron. 26 (1990) 760.

[33] A.M. McDonagh, M.P. Cifuentes, I.R. Whittall, M.G. Humphrey, M. Samoc, B. Luther-Davies, D.C.R. Hockless, J. Organomet. Chem. 526 (1996) 99.